Atomistic model of orthorhombic $YBa_2Cu_3O_7$

P. A. Deymier
Department of Materials Science and Engineering, University of Arizona, Tucson, Arizona 85721
(Received 19 January 1988; revised manuscript received 31 March 1988)

We have developed a rigid-ion model of the orthorhombic $YBa_2Cu_3O_7$ phase. The structure of the model lattice is in good agreement with available experimental structural data. The lattice is found to be unstable at 700 K where the initiation of disordering of the oxygen ions in the copper-oxygen linear chains is observed. Vibrational properties of the lattice have been calculated and compared with the experimental vibrational density of states.

INTRODUCTION

The discovery of a class of copper oxides which superconduct at temperatures above 90 K (Ref. 1) has engendered great excitement in the scientific community as well as a great deal of research activity. The superconducting phase in the Y-Ba-Cu-O mixed-phase compound was identified as $YBa_2Cu_3O_{7-x}$,[2,3] a distorted oxygen-deficient perovskite structure with the $P4/mmm$ orthorhombic space group.[4] An important feature of this structure is the existence of two-dimensional square CuO_2 layers bonded through Cu-O-Cu bonds to one-dimensional CuO_3 chains.[5] The orthorhombic cell parameters of this phase are very sensitive to the oxygen content of the perovskite structure. The oxygen stoichiometry varies in the range $0<x<1$ with the optimal superconductive temperature obtained near $x=0$.[6] The cell parameters of $YBa_2Cu_3O_7$ at room temperature are $a=3.822$ Å, $b=3.891$ Å, and $c=11.677$ Å.[7] As the oxygen content decreases an orthorhombic-to-tetragonal phase transition takes place. This is an order-disorder phase transition in which the oxygen atoms present in the Cu-O chains of the orthorhombic phase occupy sites that are normally vacant at room temperature. The transition temperature depends on the oxygen partial pressure and occurs when the stoichiometry is near $x=0.5$.[4] The tetragonal phase is not superconducting.

Although much work has gone into characterizing the properties of $YBa_2Cu_3O_{7-x}$ compounds, the mechanism of superconductivity is not established. A number of theoretical models ranging from conventional electron-phonon coupling interaction[8-10] to a variety of other mechanisms have been explored.[11-15] It has been reported that the $YBa_2Cu_3O_7$ phase shows an almost complete absence of isotope effect. The critical temperature changes only slightly upon substitution of ^{16}O by ^{18}O, providing strong evidence that phonon-mediated electron pairing is not the dominant superconductivity mechanism in this material.[16-18] Subsitution of yttrium by other rare-earth elements is also known not to change the critical temperature.[19] Absence of T_c dependence upon the isotopic mass of copper and barium has also been reported.[20]

Attempts to explain this absence of isotope effect within the conventional phonon-induced pairing theory yield unphysical values for the electron-phonon coupling parameter and the Coulomb interaction,[16] suggesting a non-phonon-pairing mechanism. The phonon spectrum of the material is the key information in making theoretical estimates for the magnitude of the isotope effect. The phonon properties of the $YBa_2Cu_3O_{7-x}$ phase have been characterized by infrared and Raman spectra.[21-23] Neutron scattering has been used to study the vibrational density of states of the superconducting $YBa_2Cu_3O_7$ as well as the nonsuperconducting $YBa_2Cu_3O_6$ phase.[24] The overall spectrum of the superconducting phase is dominated by oxygen-atom modes. The oxygens in linear-chain sites contribute to the lower-energy peaks in the spectrum and do not contribute strongly to the major feature above 360 cm^{-1}. However, in the absence of a model the authors[24] could not assign specific vibrational modes to the experimentally observed peaks.

The molecular-dynamics (MD) method is currently one of the most powerful tools for deriving the macroscopic and microscopic properties of assemblies of classical particles using realistic interatomic potentials. MD simply consists of solving the classical equations of motion of a set of interacting particles. Clearly, MD, by its own nature, provides a window on the atomic structure of the model but also provides information on its dynamics: vibrational information as well as the dynamics of processes such as phase transitions. Thermodynamics properties can be calculated as time averages along a trajectory of the system in phase space. While experimental work continues to be a major source of information about the structure and properties of materials, recent advances in the MD computational procedures may prove valuable in making a significant contribution to materials research, especially in circumstances in which either the appropriate experiments are difficult to perform accurately, or the experimental results are open to ambiguous interpretation. In that respect, MD could provide crucial clues toward the understanding of processes such as lattice phonons or orthorhombic-to-tetragonal transitions which have been shown to be critical in the study of the new superconducting oxygen-deficient perovskites.

In this paper, we present a rigid-ion model of $YBa_2Cu_3O_7$ which gives a satisfactory description of the superconducting material in constant-shape MD simulations. Structural properties of the model are computed over a wide range of temperature. The temperature dependence of order parameters describing the oxygen

sublattice in the directions a and b shows that the beginning of a disordering of the oxygen ions and vacancies in the cell base plane is taking place at 700 K. A negative thermal expansion coefficient of the lattice in the a direction confirms the instability of the oxygens in the Cu-O linear chains. Vibrational density of states of individual ions are calculated at 100 K and room temperature. The vibrational modes of the oxygen in the Cu-O linear chains exhibit a remarkable anisotropy. The oxygen vibrational modes with the lowest and highest frequency are perpendicular and parallel to the chain, respectively. The vibrational spectrum compounded from spectra of individual ions shows satisfactory agreement with the experimentally determined spectrum.

MODEL AND METHOD

The use of realistic interatomic pair potentials is critical for the generation of satisfactory MD results. For computational convenience, we have used central, pairwise additive interionic potentials to describe the interactions between ions in the oxygen-deficient perovskite. Fumi and Tosi[25] have represented the interaction between an ion i and another ion j by a pair potential of the form

$$\phi_{ij}(r_{ij}) = \frac{Z_i Z_j e^2}{4\pi\epsilon_0 r_{ij}} + A_{ij}\exp\left(-\frac{r_{ij}}{\rho_{ij}}\right) - \frac{C_{ij}}{r_{ij}^6},$$

where the total potential is the sum of a long-range Coulombic term, a short-range core-core repulsion, and a short-range van der Waals attractive term. r_{ij} is the distance between ions i and j. Z_i is the ionic charge of ion i and C_{ij} is a van der Waals attractive coefficient. The exponentially decaying repulsive term is composed of two parameters, A_{ij} and ρ_{ij}, which are characteristic of the size and "hardness" of the interacting ions.

For the simulation of the $YBa_2Cu_3O_7$ lattice, the cation-cation short-range interactions: Y-Y, Ba-Ba, Cu-Cu, Y-Ba, Y-Cu, and Ba-Cu, have been neglected. The short-range interactions for Y-O, Ba-O, Cu(1)-O, Cu(2)-O, and O-O where Cu(1) and Cu(2) are the fourfold- and fivefold-coordinated copper ions (see Fig. 1), respectively, require a set of 15 parameters. The charge on the ions, Y, Ba, Cu(1) and Cu(2), and O are taken as +3, +2, +2.333, and −2, respectively. Identical charges are assigned to all copper ions as x-ray photoemission (XPS) spectra of $YBa_2Cu_3O_7$ show one copper peak only[26] as indicated by Pauling's rules.[27] The parameters for the repulsion between Cu(1) and O and Cu(2) and O are therefore identical. The three parameters for the oxygen-oxygen short-range interaction have been taken from quantum-mechanical calculations.[28] The van der Waals coefficients for all interactions but Cu(2)-O have been set to zero. The location of the Cu(2) ions at sites with low symmetry suggests a polarization of the Cu electronic shell and therefore a strong van der Waals attraction with oxygen. The remaining seven parameters have been determined empirically by fitting the lattice parameters and interionic distances of the model to experimental values. The best set of parameters is listed in Table I.

We have applied the constant-stress molecular-dynamics formalism of Parrinello and Rahman[29] to the simulation of the assembly of Y, Ba, Cu, and O particles interacting through long-range Coulombic potentials.[30] This formalism allows for volume and shape variations of the simulation cell under periodic boundary conditions. The addition of these degrees of freedom are essential to the study of phenomena, such as phase transitions, in which volume fluctuations play a decisive role.[31]

In the constant-stress MD formulation, three variable vectors, $\mathbf{e}_1$, $\mathbf{e}_2$, and $\mathbf{e}_3$ forming a 3×3 matrix $\mathbf{H}$ are necessary to describe the planar boundaries of the simulation cell. The volume of the cell is given by $\Omega = \mathbf{e}_1 \cdot (\mathbf{e}_2 \times \mathbf{e}_3)$. The position $\mathbf{r}_i$ in a fixed Cartesian coordinate system may

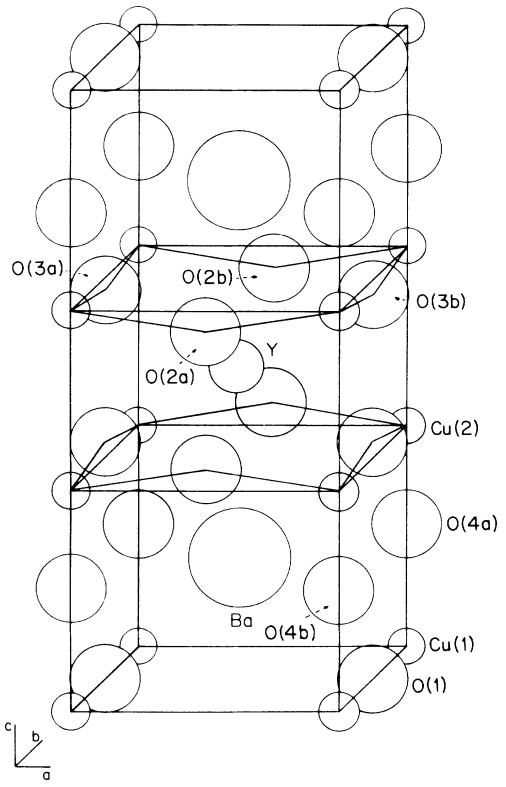

FIG. 1. Schematic of the equilibrium structure of $YBa_2Cu_3O_7$ at room temperature. The different copper and oxygen sites are shown in parentheses. Labels (a) and (b) refer to sites which are different in the model but identical in the experimental structure.

TABLE I. Parameters used in the rigid-ion model of $YBa_2Cu_3O_7$. All parameters refer to the interactions with the oxygen ions.

Ion	Z_i	$A_{iO^{2-}}$ (eV)	$\rho_{iO^{2-}}$ (Å)	$C_{iO^{2-}}$ (eV Å^6)
Y	+3	3312.0	0.278	0.00
Ba	+2	3067.2	0.335	0.00
Cu(1)	+2.333	4824.0	0.252	0.00
Cu(2)	+2.333	4824.0	0.252	38.88
O	-2	22764.3[a]	0.149[a]	20.37[a]

[a]From Ref. 28.

be expressed in the variable coordinate system as $\mathbf{s}_i = \mathbf{H}^{-1}\mathbf{r}_i$.

The edges of the simulation cell are driven by the imbalance between an externally applied stress σ and the internal stress tensor. The Lagrangian governing the equations of motion of the system under constant stress σ is written as

$$L = \tfrac{1}{2}\sum_{i=1}^{N} m_i \dot{\mathbf{s}}_i^t \mathbf{H}^t \mathbf{H} \dot{\mathbf{s}}_i - \sum_{i>j} \phi_{ij}(r_{ij}) + \tfrac{1}{2} W \mathrm{Tr}(\dot{\mathbf{H}}^t \dot{\mathbf{H}}) - \mathrm{Tr}\{\sigma\epsilon\}\Omega_0 ,$$

where $\dot{\mathbf{H}}$ stands for the time derivative of $\mathbf{H}$. $\mathbf{H}^t$ and Tr$\mathbf{H}$ are the transpose and trace of the matrix $\mathbf{H}$, respectively. The total energy is the sum of the kinetic and potential energies of the set of particles, the kinetic energy of the borders of the simulation cell to which is artificially assigned a mass W, and the elastic energy for which Ω_0 is the volume of the reference system used to measure the small strain ϵ.

The parameter W has the dimension of mass and can be visualized as the mass of the boundaries of the simulation cell. Average quantities calculated along the trajectories are independent of the mass of the borders while dynamical properties may not be. In order to generate meaningful dynamical results from MD simulations under constant-pressure conditions, a realistic choice for W can be made. [32] In this study, we have taken empirically W as five times the mass of an oxygen ion, m_{ox}. We have verified the insensitivity of the vibrational spectra of individual ions upon the mass of the boundaries in a simulation conducted with $W = 25 m_{ox}$.

The simulation of ions involves the summation of the Coulombic energy potential and forces between all pairs. The long-range nature of these interactions yields very slowly converging series. An extension to triclinic cells of the Ewald summation method[33] is incorporated into the MD algorithm to accelerate the convergence. All simulations in this study have been performed with the following set of conditions for the Ewald summation: $\eta = 5.6/L_{max}$, the real-space summations and reciprocal summations have been truncated at $r_c = \frac{1}{2} L_{min}$ and $k^2 \leq 25 \times 4\pi^2$, respectively. L_{max} and L_{min} are the longest and shortest edges of the simulation cell. The contribution of the reciprocal space energy, force, and internal stress to the total potential energy, force, and internal stress matrix is within the noise level for these quantities. Thus no further attempts were made to improve the convergence of the series in the reciprocal space.

The equations of motion generate trajectories in the isoenthalpic-isostress ensemble. The isothermal condition was implemented with a momentum-scaling procedure.[34]

We have studied a molecular-dynamics system containing nine unit cells, that is 117 ions (9 Y, 18 Ba, 27 Cu, and 63 O). The simulation cell is therefore almost cubic in shape. The system is not stable if both the shape and size of the computational cell are allowed to vary. All calculations reported in this paper are performed under constant shape conditions, that is, the borders of the simulation cell are constrained to expand only, the angle between the edges of the cell being kept at 90°.

The system was simulated under a constant external pressure of 1 atm. The equations of motion of the ions and the borders of the cell were numerically solved with a finite difference scheme. We used a time integration step of 2.68×10^{-15} sec.

RESULTS

The stability of the orthorhombic $YBa_2Cu_3O_7$ model at room temperature was checked with a simulation lasting 20000 integration steps (or 5.4×10^{-11} sec). The structure was found to be stable and only vibrational processes were observed. In particular, the oxygen ions and the oxygen vacancies remained well localized at their initial positions. The lattice parameters of the computer model at this temperature are $a = 3.819$ Å, $b = 3.883$ Å, and $c = 11.696$ Å. The model is in error by 0.25% in the a and b directions and 0.5% along the c axis. A schematic of the average structure of the $YBa_2Cu_3O_7$ model is presented in Fig. 1. One notices that the oxygen atoms in the central region of the simulation cell have relaxed and displaced toward the central plane of the cell as determined from neutron diffraction.[4] We present in Table II calculated interionic distances as well as experimental distance.[6]

The model shows very good agreement between the calculated Ba-O distances and the experimental values. Quite large differences (up to 10%) are observed in the case of Cu(1)-O(4) and Cu(2)-O(4) reflecting the fact that the copper-oxygen bonds linking the CuO_2 layers to the CuO_3 chains are of another nature than the Cu(1)-O(1) and Cu(2)-(O(2),O(3)) bonds. This result explains the relatively poor value of the c lattice parameter. The

TABLE II. Room-temperature cation-anion distances calculated from the equilibrium structure of the $YBa_2Cu_3O_7$ model. The numbers in parentheses after the ions and the labels (a) and (b) refer to particular ionic sites in the lattice as indicated in Fig. 1. The measured values are taken from Ref. 6.

Bond	Calculated (Å)	Observed (Å)	Difference (Å)
Y-O(2)	(a) 2.434	2.415	-0.019
	(b) 2.187	2.415	+0.228
Y-O(3)	(a) 2.304	2.378	+0.074
	(b) 2.267	2.378	+0.111
Ba-O(1)	2.986	2.879	-0.107
Ba-O(2)	(a) 2.967	2.976	+0.009
	(b) 3.050	2.976	-0.074
Ba-O(3)	(a) 3.010	2.970	-0.040
	(b) 2.996	2.970	-0.026
Ba-O(4)	(a) 2.724	2.743	+0.019
	(b) 2.745	2.743	-0.002
Cu(1)-O(1)	1.940	1.943	+0.003
Cu(1)-O(4)	2.110	1.850	-0.260
Cu(2)-O(2)	(a),(b) 1.967	1.928	-0.039
Cu(2)-O(3)	(a) 2.004	1.962	-0.042
	(b) 1.981	1.962	-0.019
Cu(2)-O(4)	2.065	2.303	+0.238

other copper-oxygen interionic spacings are in very good to satisfactory agreement with experimental data. Among the other differences between the calculated and measured distances, a significantly shorter yttrium-oxygen distance in some specific directions is apparent. A Y-O(3) bond shorter than that of Y-O(2) is the consequence of the orthorhombic symmetry of the cell. The computer model, however, exhibits two sets of Y-O(3) and Y-O(2) distances resulting from a distortion of the yttrium-oxygen polehydron stronger than what is really observed.

We have calculated the temperature dependence of some of the structural and thermodynamic properties of the $YBa_2Cu_3O_7$ model. Of particular interest is the temperature dependence of the cell parameters. The properties have been calculated in the interval of temperature 100–600 K. The parameters were fitted to linear temperature dependencies. The lattice parameters in Å are given by

$$a=(6.3636\times10^{-5})T+3.813,$$

$$b=-(1.1616\times10^{-5})T+3.884,$$

$$c=(1.9797\times10^{-4})T+11.676,$$

where the temperature is in K. The thermal expansion coefficient of the model in the b direction is negative, i.e., the cell contracts in that direction as temperature is raised. This result can be understood in terms of the ionic interactions. The strong van der Waals attraction of the Cu(2)-(O(2),O(3)) bonds controls the overall size of the cell parameters in the a and b directions. The oxygen ions in the Cu-O linear chains are "squeezed" between the Cu(1) copper atoms because of the large size of the barium ion. Thus the short-range core-core repulsion between Cu(1) and O(1) yields a b cell parameter larger than the a parameter. However, as thermal motion increases, the O(1) oxygen atoms are allowed to spend more time outside their tight site leading to a decrease of the cell parameter in the b direction. If we calculate by extrapolation the temperature at which both cell parameters a and b are equal, we predict that the orthorhombic $YBa_2Cu_3O_7$ phase would continuously become tetragonal at a temperature of 949 K. It is interesting to note that the experimental orthorhombic-to-tetragonal phase transition in 100% oxygen takes place at approximately 973 K.[6] However, it is important to keep in mind that the negative thermal expansion coefficient in the b direction of the model is primarily due to an increase in the amplitude of vibration of the oxygen atoms O(1) about their equilibrium positions and not to actual diffusional jumps and oxygen outgassing.

The structural changes of the orthorhombic phase upon heating have also been explored via the calculation of an oxygen-sublattice order parameter. We have defined the order parameter as

$$O_r=\frac{1}{N_{ox}}\left\langle\sum_{i=1}^{N_{ox}}\exp\{i\mathbf{k}\cdot\mathbf{r}_i\}\right\rangle,$$

where $\mathbf{k}$ is a vector in the reciprocal space, N_{ox} is the number of oxygen ions in the system, and $\mathbf{r}_i$ is the position of ion i. The $\langle\cdots\rangle$ stands for a time average calculated over a MD trajectory. A value of 1 of the parameter is characteristic of an ordered oxygen sublattice when a value of 0 is associated to a completely disordered structure. To account for the anisotropy of the lattice, two order parameters were computed by selecting the appropriate reciprocal-space vectors; the first one describes the order along the a axis when the other one orders along the b axis. The small size of the simulated system did not allow us to calculate an order parameter along the c axis. The temperature dependence of the order parameters in the interval 100–700 K is reported in Fig. 2. The sharp decrease in the order parameter along the b axis at 700 K strengthens the concept of oxygen instability in the Cu-O-Cu linear chains at high temperature. The order parameter in the a direction shows also a significant temperature dependence upon heating. The disordering is initiated by O(1) ions jumping into neighboring oxygen vacant sites. This initial step is followed by O(4) oxygen ions diffusing into the newly vacant O(1) sites which results in O(2) and O(3) ions jumping into the oxygen vacant sites located in the unit-cell midplane. The secondary oxygen jumps which occur subsequently to the initial disordering of the oxygens in the Cu-O-Cu chains are believed to be artifacts resulting from the inability of the Cu-O potentials we are using in this model to describe the interactions between the copper ions and the oxygen ions in their new environment. In order to incorporate the orthorhombic-to-tetragonal phase transition into the model, the input of Cu-O potentials varying with the oxygen coordination around the copper as well as with the symmetry of the arrangement of these oxygen ions would be required. Such an improved model would allow the study of the structure and properties of oxygen-deficient $YBa_2Cu_3O_{7-x}$.

We have calculated the temperature dependence below 700 K of some other thermodynamic properties of the computer model. The volume and enthalpy of a unit cell are given by

$$V(\text{Å}^3)=(5.2974\times10^{-3})T+172.93$$

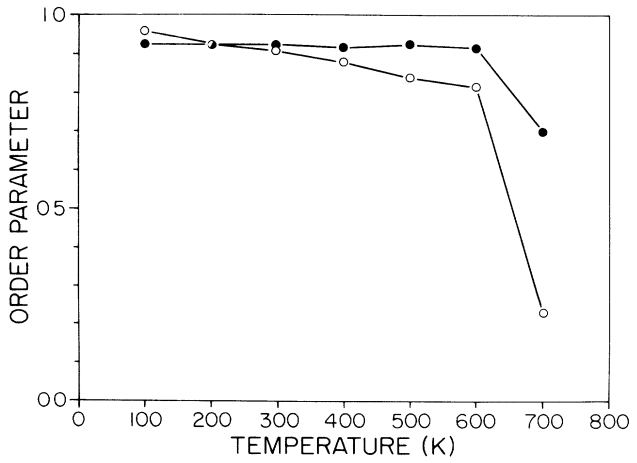

FIG. 2. Temperature dependence of the order parameters in the a and b directions. The order parameters along a and b are given as ○ and ●, respectively.

and

$$H(\text{eV}) = 0.0344T - 13.082 ,$$

where the temperature is again in K.

In addition to static or average properties, the dynamics of individual ions in the model has been explored. The velocities of Y, Ba, Cu(1), Cu(2), O(1), O(3a), and O(4) ions have been monitored during long simulations (10000 integration steps) at the two temperatures: 100 and 298 K. The oxygen atoms O(2a), O(2b), and O(3b) were not monitored as their dynamics was expected to be very similar to O(3a). O(3a) has been selected for the purpose of direct comparison with the oxygen atoms O(1). The power spectra of the components of these velocities have been calculated with a fast-Fourier-transform algorithm. The data were windowed with a Parzen window to minimize signal leakage.[35] Whenever possible, vibrational density spectra were calculated from ions far from the borders of the unit cell to avoid artifacts due to possible coupling between the simulation cell and its images. The components of the spectra at 100 K and room temperature are reported in Figs. 3 and 4, respectively. All spectra are normalized to 100. The low-energy vibrational modes of the $YBa_2Cu_3O_7$ model (below 100 cm^{-1}) are dominated by contributions from the heavy ions. Y and Ba, as well as the oxygen O(1) and copper Cu(1) when very-high-energy modes are essentially controlled by oxygen vibrations. The anisotropy of the vibrations of the O(1) ions is one of the outstanding features of the data at both low and high temperatures. All other ions show a relatively high degree of symmetry in their vibrational directions. The O(1) oxygen vibrates at frequencies as low as 50 cm^{-1} in

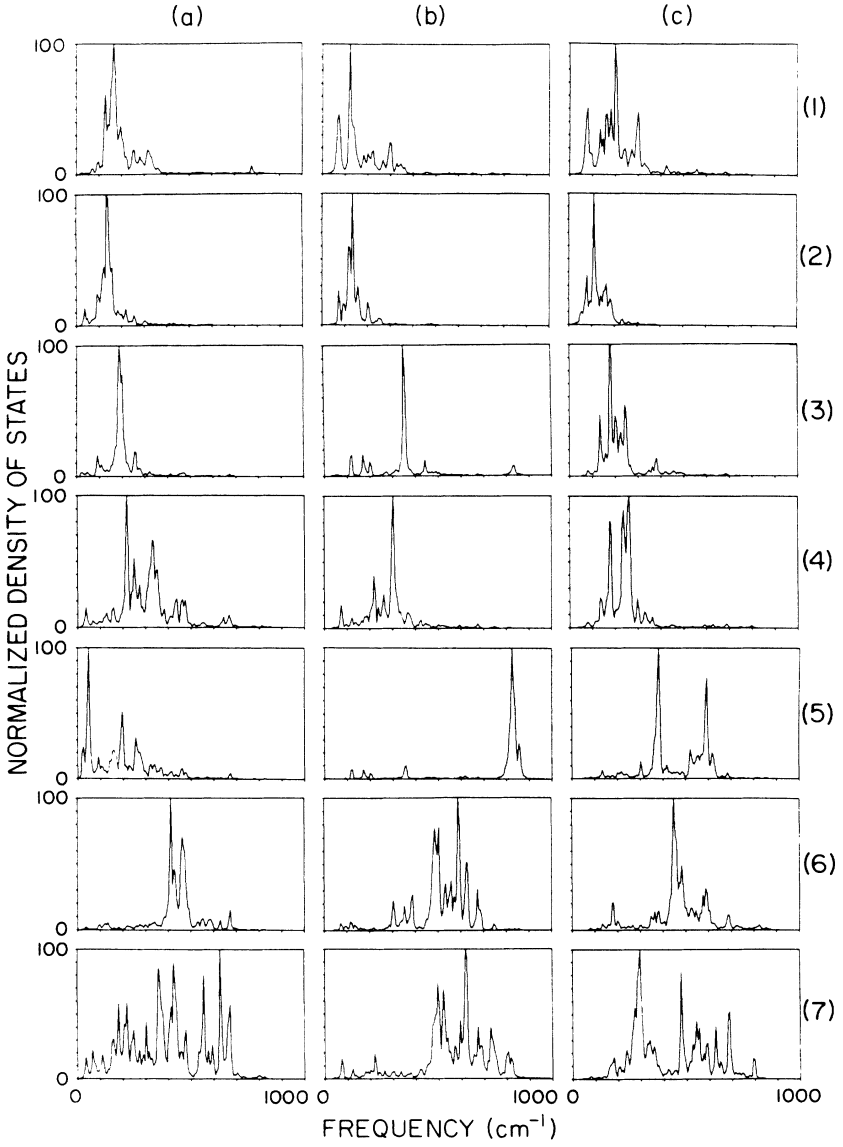

FIG. 3. Vibrational density of states at 100 K of individual ions in the directions *a*, *b*, and *c*. The densities have been normalized to their highest value. (1), (2), (3), (4), (5), (6), and (7) are referring to Y, Ba, Cu(1), Cu(2), O(1), O(4), and O(3a), respectively.

the *a* direction and as high as 820 cm^{-1} in the *b* direction. The low-frequency modes in the *a* direction of O(1) and Cu(1) are believed to be coupled modes characteristic of a transversal vibration propagating along the copper-oxygen linear chains. O(1) and Cu(1) show again a coupled vibrational mode at the very high frequency (820 cm^{-1}) which may be considered as a longitudinal mode again propagating along the linear chains. These results are characteristic of the vibrational modes in a one-dimensional two-component system.[36]

The spectra at the lowest temperature characterized by sharper peaks exhibit features similar to the high-temperature one. The coupling between the O(1) and Cu(1) ions at very low and very high frequency is weaker at the lower temperature. One also notices the sharp decrease as the temperature drops in the density of the Cu(1) vibrational mode in the *b* direction at approximately 160 cm^{-1}. The disappearance of this peak may indicate that at room temperature the Cu(1) vibrational states are coupled with the vibrational modes of the Ba ions.

Despite the absence of the information concerning the relative magnitude of the spectral components, we speculate on the general features of the vibrational density spectrum of $YBa_2Cu_3O_7$. The heavy ions as well as both types of copper ions contribute strongly to the density of states in the range 100–200 cm^{-1}. Only the vibrational modes of O(2) and O(3) contribute to the state with frequencies between 600 and 700 cm^{-1}.

Two other features in the intervals 200–300 cm^{-1} and 300–400 cm^{-1} may appear due to Cu(1) and Cu(2) modes for the former and Cu(1), Cu(2), and O(1) modes for the latter. A final major peak arising from O(4), O(2), and O(3) vibrational modes may be expected be-

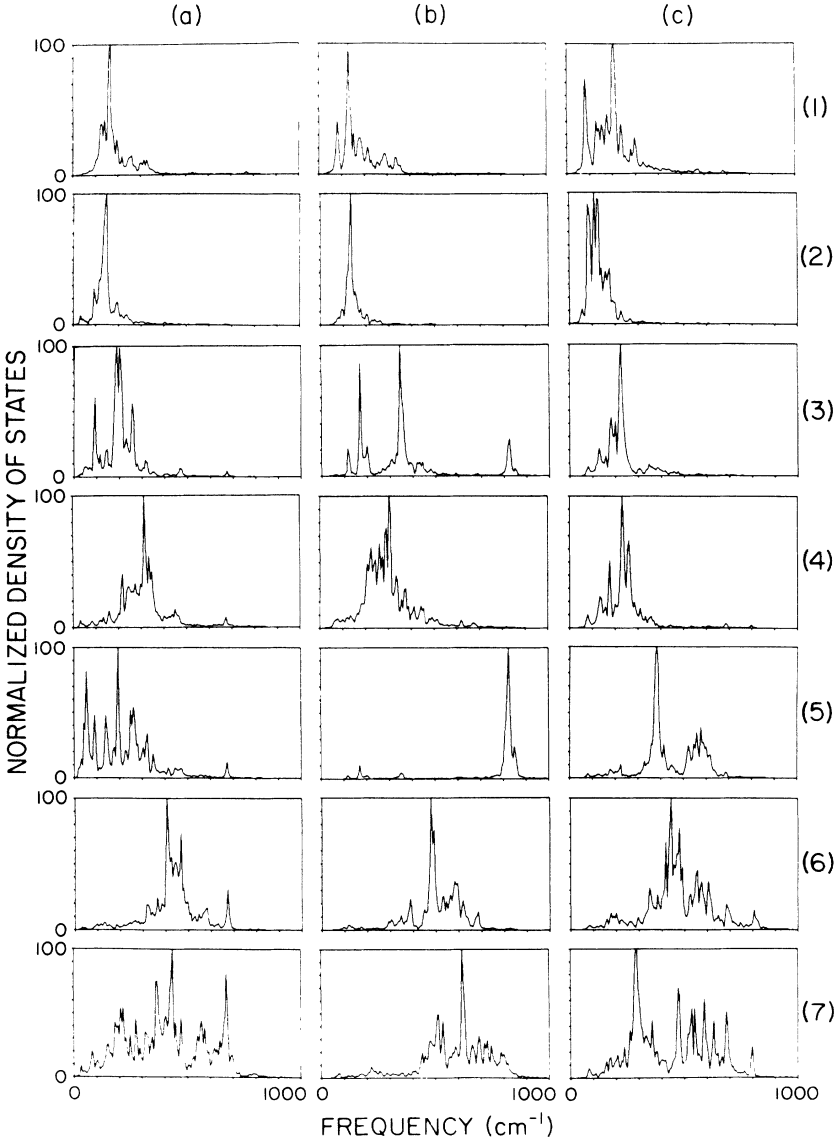

FIG. 4. Normalized vibrational density of states at room temperature of individual ions in the directions *a*, *b*, and *c*. (1), (2), (3), (4), (5), (6), and (7) are refering to Y, Ba, Cu(1), Cu(2), O(1), O(4), and O(3a), respectively.

tween 400 and 500 cm^{-1}. Because of the small number of O(1) ions only weak peaks below 100 cm^{-1} and above 800 cm^{-1} will be displayed in the global spectrum. We have calculated a model vibrational density of state by simply compounding all the computed spectra. The wave numbers at which peaks are observed are as follows: 73, 121, 133, 157, 182, 200, 218, 255, 303, 358, 382, 412, 424, 461, 479, 528, 558, 594, 631, 673, and 824. The dominant maxima are at 133, 182, 200, 255, 303, 358, 479, 558, 594, and 631 cm^{-1}.

Many peaks of the speculated spectrum are in general agreement with the vibrational density of states measured with inelastic neutron scattering at 120 K.[24] The experimental density of states reaches two large maxima near 150 and 200 cm^{-1}, followed by two other smaller maxima at about 274 and 355 cm^{-1}. Above 400 cm^{-1}, the density spectrum increases to a shoulder at 485 cm^{-1} and then a strong peak at 565 cm^{-1} before dropping to zero above 730 cm^{-1}. The most significant result is that all experimental peaks can be associated to calculated peaks within at most 19 cm^{-1}. The frequencies most in error are 133 and 255 cm^{-1}, namely vibrations of Ba in the *a* and *b* directions and Cu(2) in the *c* direction.

SUMMARY

We have been able to generate a set of interatomic potential parameters in the frame of a rigid-ion model which gives a satisfactory description of the orthorhombic $YBa_2Cu_3O_7$ phase up to 700 K. This model is, however, limited to constant-shape MD simulations. The lattice parameters of the model at room temperature as well as many interionic distances are in good agreement with experimental data. Some interionic distances, however, differ with the experimental values by as much as 10%. In particular, the distance between the copper ions and the oxygen ions in the Cu-O-Cu units linking the CuO_2 planar arrays to the CuO_3 linear chains. It is concluded that a representation of these bonds with potentials different from those used to describe to Cu-O interactions in the square planes and linear chains is needed.

The lattice model predicts a continuous change from an orthorhombic cell to a tetragonal cell at a temperature of 950 K, approximately. This change is associated with an instability at high temperature of the oxygen ions in the linear chains. The oxygen-sublattice order parameters indicate an initiation of an oxygen–oxygen-vacancy disordering at 700 K. Preliminary results on the mechanism of the initiation of disordering show that oxygen ions in the Cu-O linear chains jump to normally vacant oxygen sites. At the present time, steps of the transitions subsequent to the initiation of the disordering cannot be followed because of the inability of the current potentials to describe the phase transition.

The vibrational spectra of individual ions exhibit similar features along the *a*, *b*, *c* directions, except O(1) which possesses very anisotropic vibrational modes. No strong temperature dependence of the power spectra is observed besides the reduction at low temperature of a Cu(1)-O(1) and Cu(1)-Ba vibrational coupling. Comparison between the calculated spectra and measured vibrational density of states allowed us to make assignment of specific vibrational modes to measured peaks.

The major objective of this work was to demonstrate the feasibility of an atomistic computer model of the orthorhombic $YBa_2Cu_3O_7$ phase with a reasonable degree of realism. We believe that this model, despite its many weaknesses, may bring forth a better understanding of the new superconducting phase, $YBa_2Cu_3O_7$.

ACKNOWLEDGMENTS

The author is very grateful to the Center for Computing and Information Technology at the University of Arizona and to the College of Engineering and Mines at the same university for generous allocations of computing time. The author thanks D. Birnie III, V. Campos, and P. Phule for useful discussions and critical reading of the manuscript.

[1]M. K. Wu, J. R. Ashburn, C. J. Torng, P. H. Hor, R. L. Meng, L. Gao, Z. J. Huang, Y. Q. Wang, and C. W. Chu, Phys. Rev. Lett. **58**, 908 (1987).

[2]R. J. Cava, B. Batlogg, R. B. Van Dover, D. W. Murphy, S. Sunshine, T. Siegrist, J. P. Remeika, E. A. Rietman, S. Zahvarak, and G. P. Espinosa, Phys. Rev. Lett. **58**, 1676 (1987).

[3]P. M. Grant, R. B. Beyers, E. M. Engler, G. Lim, S. S. P. Parkin, M. L. Tamierez, V. Y. Lee, A. Nazzal, J. E. Vazyvez, and R. J. Savoy, Phys. Rev. B **35**, 7242 (1987).

[4]J. D. Jorgensen, M. A. Beno, D. G. Hinks, L. Soderholm, K. J. Volin, R. L. Hotterman, J. D. Grace, I. K. Schuller, C. U. Segree, K. Zhang, and M. S. Kleefisch, Phys. Rev. B **36**, 3608 (1987).

[5]M. A. Beno, L. Soderholm, D. W. Capone II, D. G. Hinks, J. D. Jorgensen, J. D. Grace, Ivan K. Schuller, C. U. Segree, and K. Zhang, Appl. Phys. Lett. **51**, 57 (1987).

[6]P. K. Gallagher, H. M. O'Bryan, S. A. Sunshine, and D. W. Murphy, Mater. Res. Bull. **22**, 995 (1987).

[7]R. J. Cava, B. Batlogg, C. H. Chen, E. A. Rietman, S. M. Zahurak, and D. Werder, Nature **329**, 423 (1987).

[8]W. E. Pickett, H. Krakauer, D. A. Papaconstantopoulos, and L. L. Boyer, Phys. Rev. B **35**, 7252 (1987).

[9]L. F. Mattheiss, Phys. Rev. Lett. **58**, 1028 (1987).

[10]W. Weber, Phys. Rev. Lett. **58**, 1371 (1987).

[11]K. Nasu, Phys. Rev. B **35**, 1309 (1987).

[12]A. Alexandrov and J. Ranninger, Phys. Rev. B **34**, 1164 (1987).

[13]B. K. Chakraverty, J. Phys. **42**, 1351 (1981).

[14]P. W. Anderson, Science **235**, 1196 (1987).

[15]H. B. Schuttler, M. Jarrell, and D. J. Scalapino, Phys. Rev. Lett. **58**, 1147 (1987).

[16]L. C. Bourne, A. Zettl, T. W. Barbee III, and M. L. Cohen, Phys. Rev. B **36**, 3990 (1987).

[17]L. C. Bourne, M. F. Crommie, A. Zettl, Hans-Conrad zur Loye, S. W. Keller, K. L. Leary, A. M. Stacy, K. J. Chang, M. L. Cohen, and D. E. Morris, Phys. Rev. Lett. **58**, 2337 (1987).

[18]B. Batlogg, R. J. Cava, A. Jayaraman, R. B. van Dover, G. A. Kouroukis, S. Sunshine, D. W. Murphy, L. W. Rupp, H. S. Chen, A. White, K. T. Short, A. M. Mujsce, and E. A. Rietman, Phys. Rev. Lett. **58**, 2333 (1987).

[19]D. W. Murphy, S. Sunshine, R. B. van Dover, R. J. Cava, B. Batlogg, S. M. Zahurak, and L. F. Schneemeyer, Phys. Rev. Lett. **58**, 1888 (1987); A. H. Hor, R. L. Meng, Y. Q. Wang, L. Gao, Z. J. Huang, J. Bechtold, K. Forster, and C. W. Chu, ibid. **58**, 1891 (1987).

[20]L. C. Bourne, A. Zettl, T. W. Barbee III, and M. L. Cohen (unpublished).

[21]R. J. Hemley and H. K. Mao, Phys. Rev. Lett. **58**, 2340 (1987).

[22]D. A. Bonn, J. E. Greedan, C. V. Stages, T. Timusk, M. G. Doss, S. L. Herr, K. Kamaras, and D. B. Tanner, Phys. Rev. Lett. **58**, 2249 (1987).

[23]I. Bozovic, D. Mitzi, M. Beasley, A. Kapitulnik, T. Geballe, S. Perkowitz, G. L. Carr, B. Loa, R. Sudharsaman, and S. S. Yom, Phys. Rev. B **36**, 4000 (1987).

[24]J. J. Rhyne, D. A. Neumann, J. A. Gotaas, F. Beech, L. Toth, S. Lawrence, S. Wolf, H. Osofsky, and D. U. Gubser, Phys. Rev. B **36**, 2294 (1987).

[25]F. G. Fumi and M. P. Tosi, J. Phys. Chem. Solids **25**, 31 (1964).

[26]H. Jenny *et al.* (unpublished).

[27]L. Pauling, *Nature of the Chemical Bond,* 3rd ed. (Cornell University Press, Ithaca, New York, 1960).

[28]M. J. L. Sangster and A. M. Stoneham, Atomic Energy Research Establishment, Harwell Report No. TP833, 1980 (unpublished.)

[29]M. Parrinello and A. Rahman, J. Appl. Phys. **52**, 7182 (1981).

[30]A. Rahman and M. Parrinello, in *The Physics of Superionic Conductors and Electrode Materials, NATO ASI, Odense,* edited by J. Perran (Plenum, New York, 1980).

[31]M. Parrinello, A. Rahman, and P. Vashista, Phys. Rev. Lett. **50**, 1073 (1983).

[32]H. C. Andersen, J. Chem. Phys. **72**, 2384 (1980).

[33]P. P. Ewald, Ann. Phys. (Paris) **21**, 1087 (1921).

[34]L. V. Woodcock, Chem. Phys. Lett. **10**, 257 (1971).

[35]D. F. Elliott and K. R. Rao, *Fast Transform: Algorithms, Analyses, Applications* (Academic, New York, 1982).

[36]C. Kittel, *Introduction to Solid State Physics* (Wiley, New York, 1976).